Progress In Electromagnetics Research B, Vol. 47, 37–61, 2013

ON THE SIMPLIFICATION OF THE MODELING OF ELECTRON-CYCLOTRON WAVE PROPAGATION IN THERMONUCLEAR FUSION PLASMAS

Christos Tsironis*

Department of Physics, Aristotle University of Thessaloniki, Thessaloniki 54 124, Greece

Abstract—The launching of high-frequency electromagnetic waves into fusion plasmas is an effective method for plasma heating and non-inductive current drive. In addition, the reflection of electromagnetic waves on the plasma cutoffs is utilized in electron density diagnostic measurements. The scope of this article is to comment on the standard approximations made in the simulation of electron-cyclotron wave propagation and absorption in tokamak plasmas, in connection to the established modeling tools and the underlying physics, as well as to illustrate the limits of their validity, especially regarding the applicability to ITER-related studies and beyond. The identification of possible gaps in the current state-of-the-art and the implication of new requirements for theory and modeling are also discussed.

1. INTRODUCTION

In tokamak fusion experiments, high-frequency electromagnetic waves are used in order to increase the plasma temperature, generate non-inductive current and conduct electron density measurements [1, 2]. Such waves are generated by high-power, millimeter wave sources, and their frequency is close to the electron-cyclotron (EC) frequency or one of its harmonics, so that they are resonantly absorbed by the plasma electrons [3]. Depending on the angle of propagation at resonance, the absorbed wave power is divided to the electron motions perpendicular and parallel to the magnetic field. The former part results to plasma heating, whereas the latter one excites electron current in the plasma. Electron-cyclotron current drive (ECCD) is used for suppressing magnetohydrodynamic (MHD) instabilities like

Received 29 October 2012, Accepted 12 December 2012, Scheduled 12 December 2012
* Corresponding author: Christos Tsironis (ctsironis@astro.auth.gr).

neoclassical tearing modes (NTMs) [4], whereas it is also important for tokamak steady-state operation. Since the cyclotron frequency is proportional to the magnetic field, which is non-uniform in fusion devices [5], the resonance condition is realized in a narrow spatial region and good localization of the energy deposition requires the injection of the wave power in the form of focused beams.

With respect to the theory and modeling, the problem of electron-cyclotron heating may be divided into two different parts: The problem of the wave propagation and absorption (effect of the plasma on the wave) and the problem of the evolution of the electron distribution function (wave effect on the plasma) [6]. One usually treats each part of the problem separately, while a coupling of the two parts constitutes the core of a self-consistent treatment (see, e.g., [7, 8]). For our interest, the problem of wave propagation and absorption is straightly connected to the solution of Maxwell's equations. In problems involving realistic wave and plasma geometry, a numerical treatment is unavoidable due to the complicated form of the associated equations.

When the wavelength is small compared to the medium inhomogeneity, which is frequently the situation in fusion experiments, a simplification is achieved by using asymptotic methods [9]. The most applied of these methods is geometric optics (ray tracing) [10, 11], where the solution is simplified to canonical equations with the dispersion function playing the role of the Hamiltonian. Ray tracing provides a direct physical picture in terms of wave rays, however the results become questionable in the case of focused beams since typical wave effects are neglected in this approach. Asymptotic methods which incorporate wave effects to geometric optics are quasi-optical beam tracing [12, 13], which includes an intermediate-order term in the dispersion relation for the description of the beam spanning across propagation, and paraxial beam tracing [14], which retains the ray tracing description along the propagation while across it solves for the beam profile taking into account diffraction.

In cases where the aforementioned short-wavelength limit breaks down, the treatment of relevant issues should be pursued in the frame of a full-wave solution. The main reason is that, in terms of modeling, wave effects are connected to the appearance of additional wave modes, coming from Maxwell's equations, due to the rapid spatial change of the wavenumber. This behavior, along with mode purity and polarization, cannot be described in terms of conventional geometric optics. A numerical method potential to provide a full-wave solution is the Finite-Difference Time-Domain (FDTD) method [15], where Maxwell's equations are transformed into a set of finite-difference equations on a grid such that the Faraday and Ampere laws are always valid. Despite

the advantages of FDTD, there has been little application in fusion plasmas up to now due to the high computational demands [16, 17].

Apart from the wave description, the modeling of the plasma medium introduces further approximations. Most solvers assume linear cold plasma dispersion for the real part of the wavenumber (describing the wave propagation) near and far from resonance, and the imaginary part, which describes cyclotron damping, is computed from the complex dispersion relation only in the resonance area [6]. Furthermore, the assumption of weak absorption is adopted, where the imaginary wavenumber is considered an order of magnitude smaller that the real part [10]. The above are motivated by the fact that, for parameters relevant to modern devices, the wave intensity is very small and, apart from the narrow resonance region, the wave-plasma coupling is very weak. However, the direction of propagation, the localization of the deposition and the amount of absorbed power can differ a lot from the ones implied by the linear cold plasma model when the electron temperature is very high, e.g., relevant to DEMO. In such cases, the plasma response should include high temperature effects and, in some cases, also nonlinear wave-particle interaction (as, e.g., in [18]).

Other effects that involve both the wave and plasma ought to be accounted for, as, e.g., the role of the magnetic field configuration on ECRH/ECCD through the modification of the plasma response characteristics. In some cases, it may be important to address the actual tokamak equilibrium, also in the presence of MHD instabilities which result to the appearance of magnetic islands. Since ECRH/ECCD is used for the control/suppression of such phenomena, it may be also crucial to estimate the effect of the presence of islands on the power absorption and current drive [19, 20]. A second issue is related to the description of the transformation of the initially assumed Gaussian wave beam to a more complicated wave object due to localization, asymmetry and inhomogeneity in the absorption. For this issue, it would be advantageous to describe modifications of the beam profile in terms of the generation of interacting higher-order Gaussian modes.

There are several codes implementing the methods just described (indicatively we mention [21–23]), and the results are in partial agreement with a number of dedicated experiments [2, 24]. In this paper, we address the validity of the commonly-made simplifications and analyze the possible alternatives for future reactor modeling. The most important issues, on which we primarily focus, are: (i) The reliability of asymptotic methods as the short-wavelength-limit parameter approaches unity, (ii) the limits of validity of the weakly-inhomogeneous medium description, (iii) the applicability of the cold

plasma model for high-temperature reactors, (iv) the consistency of the constantly-Gaussian beam assumption, and (v) the inaccuracy induced from the use of approximate equilibria in wave codes.

The structure of the paper is as follows: In Section 2, the conventional theory of high-frequency wave propagation in plasmas is summarized, and in Section 3, the limits of validity of methods emanating from geometric optics are discussed. Then, in Section 4, the consistency of adopting the cold plasma model in the description of wave propagation in high-temperature plasmas is analyzed, and in Section 5, the accuracy of the assumption that a high-frequency beam remains Gaussian during propagation is studied. In Section 6, the dependence of the wave propagation on the plasma equilibrium details is examined, and the last section summarizes the discussion on the cases where conventional tools fail to provide a reliable solution.

2. THEORY OF PLASMA WAVE PROPAGATION

The basis for any treatment on electromagnetic wave propagation in magnetized plasmas relies on Maxwell's equations or the vector wave equation (a separate one for each field), which provide a more direct description of the propagation [3, 6]. In their general form, these read

$$\begin{aligned} \nabla^2 \bar{E} - \frac{1}{c^2}\frac{\partial^2 \bar{E}}{\partial t^2} &= \frac{\nabla \rho}{\epsilon_0} + \mu_0 \frac{\partial \bar{j}}{\partial t} \\ \nabla^2 \bar{B} - \frac{1}{c^2}\frac{\partial^2 \bar{B}}{\partial t^2} &= \mu_0 \nabla \times \bar{j} \end{aligned} \tag{1}$$

where $\bar{E}(\bar{r}, t)$, $\bar{B}(\bar{r}, t)$ are respectively the electric and magnetic field, and $\rho(\bar{r}, t)$, $\bar{j}(\bar{r}, t)$ are the volume densities of the charge and current sources in the plasma, whereas ϵ_0, μ_0 and c are the electric permittivity, magnetic permeability and speed of light in vacuum.

The presence of ρ, $\bar{j}$ in (1) raises the need for a model of the plasma response. In general, since the plasma is actually a collection of charges and currents in vacuum, the description of the source terms is according to microscopic plasma dynamics:

$$\begin{aligned} \rho(\bar{r}, t) &= \lim_{\Delta V \to 0} \frac{1}{\Delta V} \sum_j q_j(\bar{r}_j, t)\delta(\bar{r} - \bar{r}_j) \\ \bar{j}(\bar{r}, t) &= \lim_{\Delta V \to 0} \frac{1}{\Delta V} \sum_j q_j(\bar{r}_j, t)\bar{\mathrm{v}}_j(t)\delta(\bar{r} - \bar{r}_j) \end{aligned} \tag{2}$$

with $\bar{r}_j$, $\bar{\mathrm{v}}_j$ the position and velocity of the electric charge q_j and ΔV a small volume around $\bar{r}$. The general case is that the solution depends nonlinearly on the source terms. The special case $\rho = \bar{j} = 0$ yields

propagation in vacuum, where the wave transmits on a straight line path with a planar phase front and the fields are transverse to the direction of propagation and harmonic in time and space

$$\bar{E}(\bar{r},t) = \bar{A}\exp\left[i\left(\bar{k}\cdot\bar{r}-\omega t\right)\right] \tag{3}$$

In (3), $\bar{A}$ is the wave amplitude and $\varphi = \bar{k}\cdot\bar{r}-\omega t$ the phase. Another notable case for applications is the weak-field limit, where the plasma dynamics linearly depends on the electric field. In this case, the source terms are given by $\rho = \nabla(\tilde{\epsilon}\cdot\bar{E})$ and $\bar{j} = \tilde{\sigma}\cdot\bar{E}$, where $\tilde{\varepsilon}(\bar{r},\bar{k}) = \tilde{\epsilon}(\bar{r},\bar{k}) + i\omega^{-1}\tilde{\sigma}(\bar{r},\bar{k})$ is the effective complex dielectric tensor describing the plasma medium permittivity and conductivity.

The complexity in tokamak geometry makes a full-wave solution hard to obtain. For the typical parameters met in the experiment, a simplified treatment can be followed in terms of frequency-domain asymptotic methods for constant-frequency wave in linear and stationary plasma. This theory is based on the fact that if the plasma parameters that affect propagation (density, temperature and magnetic field) vary much slower in space than the wave phase, the plane-wave ansatz can be generalized to provide an approximate local solution of the wave equation. This is quantified by the condition $\kappa = \lambda^{-1}L \gg 1$, where $L = \min(\langle|\nabla\xi|/\xi\rangle^{-1})$ $(\xi = n, T, B)$ is the smallest inverse mean plasma gradient and λ the wavelength. In this framework, the wave equation for the electric field reduces to the Helmholtz equation [3, 10]

$$\nabla\times\nabla\times\bar{E} - \frac{\omega^2}{c^2}\tilde{\varepsilon}\cdot\bar{E} = 0 \tag{4}$$

and the expression for the spatial part of $\bar{E}$ stems from the one in (3), with a generalized phase $\varphi(\bar{r},t) = \kappa s(\bar{r}) - \omega t$ based on $\bar{k} = \kappa\nabla s$

$$\bar{E}(\bar{r}) = \bar{A}(\bar{r})\exp[i\kappa s(\bar{r})] \tag{5}$$

The gain from applying asymptotic methods is the reduction of the wave equation to a more tractable set of canonical equations. This is formulated with the expansion of the electric field amplitude in an asymptotic series over the parameter κ, followed by the insertion of the series in (4), the classification of the terms of different order in separate equations and the solution of these equations [9]. The weak spatial variation imposes the additional rule that the effect of absorption on the dispersion is of lower order, reflected in $\tilde{\varepsilon} = \tilde{\varepsilon}^H + i\kappa^{-1}\tilde{\varepsilon}^A$, where $\tilde{\varepsilon}^H$, $\tilde{\varepsilon}^A$ are the Hermitian and anti-Hermitian part of $\tilde{\varepsilon}$. Depending on the specific ansatzes for the eikonal s and the amplitude series, there are three different asymptotic methods applied to fusion problems: Ray tracing, emanating from geometric optics, quasi-optical ray tracing and paraxial beam tracing, products of the complex eikonal theory.

The pioneer asymptotic method is geometric optics, or ray tracing [9–11]. Within this technique, the propagation is described by the trajectories of one or more non-interacting wave rays which are continuously refracted by a weakly-inhomogeneous medium, in the same way as the trajectory of a particle is deflected by a scalar potential. The electric field ansatz is a generalization of the standard plane wave, and for each ray one can determine the backbone of the wave field by calculating the variation of the phase and the amplitude along its path. The relevant equations are obtained as described above, by exploiting the asymptotic series expansion of the amplitude

$$\bar{A} = \sum_j \kappa^{-j} \bar{A}_j \tag{6}$$

inserting (5), (6) in (4) and separating terms of different order in κ. The zero-order equation yields the dispersion relation

$$\left[\frac{c^2}{\omega^2} \left(-k^2 \bar{I} + \bar{k} \star \bar{k} \right) + \tilde{\varepsilon}^H \right] \cdot \bar{A}_0 \equiv \tilde{\Lambda} \cdot \bar{A}_0 = 0 \tag{7}$$

The solvability condition $\det(\tilde{\Lambda}) \equiv H(\bar{r}, \bar{k}) = 0$ is a Hamilton-Jacobi equation with respect to s over a parameter τ along the ray. This results to Hamiltonian equations which trace the evolution of the ray trajectory and the local value of the wavenumber in the plasma

$$\begin{aligned} \frac{d\bar{r}}{d\tau} &= \frac{\partial H}{\partial \bar{k}} \\ \frac{d\bar{k}}{d\tau} &= -\frac{\partial H}{\partial \bar{r}} \end{aligned} \tag{8}$$

The first-order equation gives the amplitude evolution along the ray

$$\frac{d|\bar{A}_0|^2}{d\tau} = -\left(\nabla \cdot \bar{v}_g + 2\alpha_L \right) |\bar{A}_0|^2 \tag{9}$$

where $\bar{v}_g = \partial H / \partial \bar{k}$ is the group velocity, $\alpha_L = \bar{e^*} \cdot \tilde{\varepsilon}^A \cdot \bar{e}$ the absorption coefficient and $\bar{e}$ the polarization vector ($\bar{A}_0 = A_0 \bar{e}$). (9) implies that the wave energy propagates in the direction of the group velocity and that the absorption is proportional to the projection of the anti-Hermitian part of the dielectric tensor onto the polarization vector.

The ray tracing approach provides a valuable tool to solve the wave equation for high-frequency electromagnetic waves. However, there is an important limitation that crucial wave phenomena, like interference and diffraction, are not included in the description. Within the formulation of geometric optics, any interaction between the rays is considered to be weaker than dispersion and appears only in the higher-order equations, which are difficult to treat. In cases where such effects

cannot be neglected, the application of ray tracing brings up physical inconsistencies near foci or caustics. This has led to the development of more advanced asymptotic methods that refine geometric optics, taking into account wave effects, in order to deal with the beam width variation due to the diffractive broadening of the beam cross-section.

Quasi-optical ray tracing, based on the complex eikonal theory, is historically the first method to handle the aforementioned issue [12, 13]. The innovation with respect to standard geometric optics is in the replacement of s with a more general, complex eikonal function $\psi = s + i\phi$, where the imaginary wavevector is perpendicular to the group velocity. The ansatz of (5) then becomes

$$\bar{E}(\bar{r}) = \bar{A}(\bar{r}) \exp[-\kappa\phi(\bar{r})] \exp[i\kappa s(\bar{r})] \tag{10}$$

where the first exponential describes the distribution of the electric field on the plane transverse to the propagation. In this context, an intermediate length scale between λ and L comes into play, the beam width W. Due to the Fresnel condition $W^2 \geq \lambda L$ [12], the imaginary wavenumber scales as W^{-1} and is of order $\kappa^{-1/2}$ with respect to the real part. Following the standard geometric optics formalism but using the field ansatz in (10), the solutions for the ray trajectories turn out complex-valued because the Hamiltonian is itself complex. This may be overcome via a Taylor expansion of the complex dispersion function according to the inequality $\Im(\bar{k}) \ll \Re(\bar{k})$.

The emergent Hamiltonian consists only of real-valued terms, the zero-order one of geometric optics and one of intermediate-order that describes wave effects (the imaginary term $\Im(\bar{k}) \cdot \bar{v}_g$ equals to zero)

$$H(\bar{k}) = H\left[\Re(\bar{k})\right] - \frac{1}{2} \sum_{\alpha,\beta} \Im(k_\alpha)\Im(k_\beta) \frac{\partial^2 H\left[\Re(\bar{k})\right]}{\partial\Re(k_\alpha)\partial\Re(k_\beta)} \tag{11}$$

where the Greek-letter summation indices refer to the Cartesian coordinate system. Using this Hamiltonian it is straight forward to obtain the quasi-optical ray equations [13], one for the ray position and two for the real and imaginary part of the wavenumber. These update the previously derived description of the propagation including additional ray bending with respect to the one calculated from ray tracing, in terms of the effect of neighboring rays which is modeled by the terms of half-order. In this framework, wave diffraction is interpreted as the effect of an energy flux transverse to the geometric-optics rays, driven by the interactions between the rays.

The last approach to mention is paraxial beam tracing [14], where the electric field ansatz is the same as in (10), however the amplitude series is different: The whole amplitude term is first expanded into Gaussian-Hermite modes, with result $\bar{A}\exp(-\kappa\phi) = \sum_{mn} \bar{E}_{mn}$, each

one of which is then asymptotically expanded with the inclusion of additional terms of intermediate order:

$$\bar{\mathbb{E}}_{mn} = \Phi_{mn}\bar{A}_0 - i\kappa^{-1/2}\sum_j \frac{\partial \Phi_{mn}}{\partial \xi_j}\bar{A}_1^j - \kappa^{-1}\left(\frac{1}{2}\sum_{j,l}\frac{\partial^2 \Phi_{mn}}{\partial \xi_j \partial \xi_l}\bar{A}_2^{jl} - i\Phi_{mn}\bar{A}_3\right) \quad (12)$$

A dimensionless coordinate system (τ, ξ_1, ξ_2) is associated with the beam (see Fig. 1), where $\xi_1,\ \xi_2$ are local coordinates on the plane where the beam profile spans. The curve $\xi_1 = \xi_2 = 0$ is a geometric-optics ray that describes the beam axis, whereas the functions $\Phi_{mn}(\xi_1, \xi_2) = H_m(\xi_1)H_n(\xi_2)\exp[-(\xi_1^2 + \xi_2^2)/2]$ describe the beam profile.

The determination of the wave-front and the beam cross-section requires the calculation of the complex eikonal ψ. Since narrow beams are used, the electric field is negligent at distances from the beam axis larger than $3W$. This allows to simplify by a Taylor expansion in space around the axial ray. Since $\Im(\bar{k}) \cdot \bar{v}_g = 0$, the expansion is written as

$$\psi = \psi(\bar{r}_0) + \frac{1}{2}\frac{\partial^2 \psi}{\partial r_\alpha \partial r_\beta}(r_\alpha - r_{0\alpha})(r_\beta - r_{0\beta}) \quad (13)$$

The coefficients $\psi_{\alpha\beta} = \partial^2\psi/\partial r_\alpha \partial r_\beta$ are determined by an ordinary differential equation emerging from the terms of order $\kappa^{-1/2}$ [14]

$$\frac{d\psi_{\alpha\beta}}{d\tau} = -\frac{\partial^2 H}{\partial r_\alpha \partial r_\beta} - \sum_\gamma\left(\frac{\partial^2 H}{\partial r_\beta \partial k_\gamma}\psi_{\alpha\gamma} - \frac{\partial^2 H}{\partial r_\alpha \partial k_\gamma}\psi_{\beta\gamma}\right) - \sum_{\gamma,\delta}\frac{\partial^2 H}{\partial k_\gamma \partial k_\delta}\psi_{\alpha\gamma}\psi_{\beta\delta} \quad (14)$$

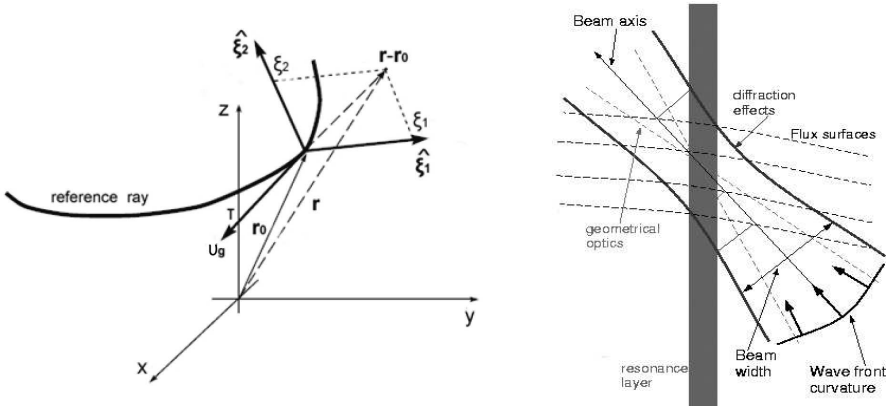

(a) (b)

Figure 1. Illustration of the local wave ray and beam representation.

The real part of $\psi_{\alpha\beta}$ is related to the wave-front curvature by $s_{\alpha\beta} \propto R_c^{-1}$ and the imaginary part scales with the beam width as $\phi_{\alpha\beta} \propto W^{-2}$. In a proper coordinate system where s, ϕ become diagonal, their nontrivial elements provide these beam parameters in the directions transverse to propagation. The amplitude transport is again given by (9), however absorption is calculated on the central ray but refers to the whole beam. For this reason, the amplitude solution is build up from $\bar{A}_0$ excluding the Gouy shift with respect to the beam axis [25]

$$\Theta_{mn}=\int_0^{\tau} d\tau \sum_{\alpha,\beta} \frac{\partial^2 H}{\partial k_\alpha \partial k_\beta}\left[\left(m+\frac{1}{2}\right)\frac{\partial \xi_1}{\partial r_\alpha}\frac{\partial \xi_1}{\partial r_\beta}+\left(n+\frac{1}{2}\right)\frac{\partial \xi_2}{\partial r_\alpha}\frac{\partial \xi_2}{\partial r_\beta}\right] \tag{15}$$

Given a model for the plasma, the medium response can be determined and the propagation problem is in principle then solved. In the linear regime, where the response is suitably expressed in terms of a generalized dielectric medium, it is feasible to connect the permittivity and conductivity tensors to the plasma dynamics by a term-to-term comparison of the coefficients of $\bar{E}$ in the relation $\bar{j} = \tilde{\sigma} \cdot \bar{E}$, after $\bar{j}$ has been calculated from the linearization of the plasma model. A complete model for the plasma should trace the charged particles under the effect of all electromagnetic fields, which is practically impossible. The most realistic from the simplified models is kinetic theory, based on Vlasov's equation for the particle distribution function $f(\bar{r}, \bar{p}, t)$ [26]

$$\frac{\partial f}{\partial t} + \bar{\mathrm{v}} \cdot \frac{\partial f}{\partial \bar{r}} + q\left(\bar{E} + \bar{\mathrm{v}} \times \bar{B}\right) \cdot \frac{\partial f}{\partial \bar{p}} = 0 \tag{16}$$

Solutions relevant to dynamic equilibrium do not depend on time ($\partial f/\partial t = 0$) and, for homogeneous equilibria, also on space ($\nabla f = 0$).

In the frame described above, different assumptions may yield a different implementation of the dielectric tensor. It is beyond the scope of this article to go into the details of the calculations, here only the main steps are sketched: (a) Linearize Vlasov's equation assuming homogeneous static equilibrium plus a small-amplitude perturbation, (b) solve for the distribution function by integrating along the unperturbed orbits in velocity space, (c) calculate the current density as the first-order moment of the distribution. The result is:

$$\frac{\tilde{\varepsilon}}{\epsilon_0} = \tilde{I} + \frac{\omega_p^2}{\omega} \sum_{l=-\infty}^{\infty} \int \frac{d^3p \frac{1}{\gamma p}\frac{df_0}{dp}}{\omega - k_{||}\mathrm{v}_{||} - \frac{\mathrm{l}\omega_c}{\gamma}} \begin{bmatrix} \frac{l^2}{b^2}J_l^2 p_\perp^2 & i\frac{l}{b}J_l J_l' p_\perp^2 & \frac{l}{b}J_l^2 p_{||} p_\perp \\ -i\frac{l}{b}J_l J_l' p_\perp^2 & (J_l')^2 p_\perp^2 & -iJ_l J_l' p_{||} p_\perp \\ \frac{l}{b}J_l^2 p_{||} p_\perp & iJ_l J_l' p_{||} p_\perp & J_l^2 p_{||}^2 \end{bmatrix} \tag{17}$$

In the above, $\omega_p^2 = \epsilon_0 n_e/m_e$ is the plasma frequency, f_0 the equilibrium distribution function, $J_l(b)$ the Bessel function of order l and argument $b = k_\perp p_\perp (m_e\omega_c)^{-1}$, and $\omega_c = q_e B_0/m_e$ the cyclotron frequency.

In order to derive an exact expression for the kinetic (hot) plasma dielectric tensor, one has to insert Maxwell's distribution as f_0 in (17) and perform the integrations. In the fully-relativistic case, the evaluation requires numerical effort from a point on, so for achieving analytic expressions one should resort to approximations. For plasma temperatures within the weakly-relativistic limit, a Taylor expansion employed in the Lorentz factor makes feasible the analytic evaluation of the velocity-space integrals. The non-relativistic approximation amounts to setting $\gamma = 1$ and using the classical version of Maxwell's distribution, which allows for the integration over $p_{||}$ to be carried out analytically. The validity of this approach requires that the resonant electrons remain sub-relativistic. Far from resonances and cutoffs, one may adopt the fluid (cold) plasma description by setting $\bar{p} = 0$ in (17).

For determining the frequency spectrum of allowed propagation, it is sufficient to analyze the dispersion relation rather than fully solve the wave equation. The linear modes of interest for fusion are the linearly-polarized O-mode and the elliptically-polarized X-mode [3, 5]. Cold-plasma dispersion suggests that the O-mode does not depend on the magnetic field, thus the wave appears only the cutoff at the plasma frequency. In tokamaks, the density and temperature increase from the edge to the center and the magnetic field rises along the propagation. This places the cutoffs for the O-mode close to the plasma center [2]. Moreover, within the kinetic model, the hot-plasma dispersion relation describes damping consistently through the imaginary part of the wavenumber, which is equal to the absorption coefficient.

3. LIMIT OF VALIDITY OF ASYMPTOTIC METHODS

The state-of-the-art in the theoretical tools for the simulation of EC wave propagation in fusion devices, which is based on asymptotic methods in a large degree, is sophisticated and generally considered reliable for ITER modeling as well as for preliminary DEMO studies. The established ray/beam tracing codes have been benchmarked successfully in ensuring the validity of the physics models and their implementation in the numerical codes, as well as in providing a deeper understanding in cases where disagreement was found [2].

In standard geometric optics, only the two lowest-order equations from the whole hierarchy are retained: Zero-order describes the wave dispersion, which is independent of the amplitude, whereas first-order provides the amplitude evolution involving only the zero-order term, assuming $\kappa^{-j}\bar{A}_j \ll \bar{A}_0$ in (6). However, investigating the higher-order terms is important since diffraction appears only in higher-order. Moreover, solutions based on geometric optics become

questionable beyond the limit $\kappa \approx 1$, where the asymptotic series fails to converge because all higher-order terms become sizeable for the amplitude calculation. The importance of the higher-order terms in the asymptotic expansion has been studied in the past from the scope of the robustness of the zero-order description in geometric optics [9].

The analysis of the contribution of the higher-order terms starts with the derivation of the whole hierarchy of equations described above. With reference to [10], our purpose requires that we include also the second-order terms in the expression of the current density. This reads

$$\bar{j} = i\omega \left[- \left(\tilde{\varepsilon}^H - \epsilon_0 \tilde{I} \right) \cdot \bar{A} + \kappa^{-1} \tilde{K}_1(\bar{A}) + \kappa^{-2} \tilde{K}_2(\bar{A}) \right] \tag{18}$$

where the terms $\tilde{K}_1(\bar{A})$, $\tilde{K}_2(\bar{A})$ are given by

$$\begin{aligned} \tilde{K}_1(\bar{A}) &= i\tilde{\varepsilon}^A \cdot \bar{A} - \frac{1}{2} \left[\frac{\partial}{\partial \bar{r}} \left(\frac{\partial \tilde{\varepsilon}^H}{\partial \bar{k}} \right) \right] \cdot \bar{A} + \frac{\partial \tilde{\varepsilon}^H}{\partial \bar{k}} \cdot \frac{\partial \bar{A}}{\partial \bar{r}} \\ \tilde{K}_2(\bar{A}) &= \frac{1}{2} \left[\frac{\partial}{\partial \bar{r}} \left(\frac{\partial \tilde{\varepsilon}^A}{\partial \bar{k}} \right) \right] \cdot \bar{A} - \frac{\partial \tilde{\varepsilon}^A}{\partial \bar{k}} \cdot \frac{\partial \bar{A}}{\partial \bar{r}} \end{aligned} \tag{19}$$

The sequence of actions for obtaining the intermediate equations of geometric optics yields the following relation in order n:

$$i\tilde{\Lambda} \cdot \bar{A}_n = -\Delta_n^0 \left[\nabla \cdot \left(\bar{k} \times \bar{A}_{n-1} \right) + \bar{k} \times \left(\nabla \times \bar{A}_{n-1} \right) - \tilde{K}_1 \left(\bar{A}_{n-1} \right) - \Delta_n^1 \tilde{K}_2 \left(\bar{A}_{n-1} \right) \right] \tag{20}$$

In the above, $\Delta_l^m = 1 - \delta_l^m$ is the complement of the Kronecker delta. Clearly for $n = 0$ and 1 one obtains the intermediate equations in zero and first order, from which (7) and (9) are derived (for more details see, e.g., [10, 11]). The amplitude terms of higher-order may be calculated iteratively using (20), as it is already in the form $\tilde{\Lambda} \cdot \bar{A}_n = \tilde{\Omega}(\bar{A}_{n-1})$, or by derivation and solution of a separate transport equation for each $\bar{A}_n$, in analogy to (9). This exact computation is beyond the scope of this article and will be treated in a future work.

Since the zero-order result does not depend on the amplitude, as κ approaches 1 its validity is not affected by any higher-order corrections but only from the gradual inability to distinguish consistently between the different orders, which however occurs for values of κ closer to 1. This is referred to as the "zero-order accuracy" of geometric optics and allows the methods to be robust in computing the propagation path in cases where κ takes values not much higher than 1. This property has been first pointed out in [9], and its validity has been illustrated in fusion applications involving such "grey-area" parameters [27, 28]. In these cases, the accuracy of the amplitude calculation may be also redeemed if a number of higher-order terms are included in the result.

A quantification of the limits where asymptotic methods are valid is established according to the tolerance for the series accuracy and its comparison to the exact value of κ, which is determined by the wave frequency and the spatial profiles of the plasma parameters. Reminding that κ^{-1} is the ratio between two amplitude terms of adjacent order, by keeping n_r terms the achieved accuracy with respect to zero-order is κ^{-n_r}. If the minimum for the order of accuracy is n_1 and the maximum is n_2, the condition for quasivalidity is respectively $10^{-n_2} \leq \kappa^{-n_{\rm qv}} \leq 10^{-n_1}$, or solved after the required number of terms

$$\mathrm{int}\left(\frac{n_1}{\log\kappa}\right) \leq n_{qv} \leq \mathrm{int}\left(\frac{n_2}{\log\kappa}\right) \tag{21}$$

Evidently, (21) provides the minimum number of terms to be kept for geometric optics to be valid without controversy, as well as the region of parameters where the results should be examined more thoroughly.

For all cases where $\kappa > 10^{n_2}$ the validity of asymptotic tools is preserved within zero-order, since $\min(n_{\rm qv}) = 0$, with accuracy of order n_2. On the contrary, $\kappa \simeq 1$ leads to breakdown because a very large number of terms is required to achieve any order of accuracy. There can be different choices for a consistent definition of the accuracy limits. Indicatively, one may define n_1, n_2 in terms of the degree of convergence of the amplitude series, or on the basis of the error with respect to a full-wave solution. More specialized definitions may be based on the requirements of the specific experiment to be simulated. For example, in problems where accurate power deposition is required, a minimum error in the distance from the target and a good estimation of the absorbed power need to be achieved, which translate (through dimensional analysis) in allowed errors for the electric amplitude.

We analyze characteristic cases of interest for ITER ECRH. Regarding the parameters involved, $\omega/2\pi = 170\,\mathrm{GHz}$ (relevant to the fundamental-harmonic O-mode), and the plasma profiles:

$$\begin{aligned} B_0(r) &= B_0(0)\frac{r_{\rm maj}}{r_{\rm maj}+r} \\ n_e(r) &= n_e(0) - [n_e(0) - n_e(r_{\rm min})]\left(\frac{r}{r_{\rm min}}\right)^2 \end{aligned} \tag{22}$$

with $r_{\rm maj} = 6.2\,\mathrm{m}$, $r_{\rm min} = 1.9\,\mathrm{m}$ the major and minor plasma radius, $B_0(0) = 5.3\,\mathrm{T}$ the magnetic field at the plasma centre and $n_e(0) = 10^{14}\,\mathrm{cm}^{-3}$, $n_e(r_{\rm min}) = 10^{13}\,\mathrm{cm}^{-3}$ the density at the plasma centre and edge. The temperature has a profile similar to the one of the density with $T_e(0) = 10\,\mathrm{keV}$, $T_e(r_{\rm min}) = 1\,\mathrm{keV}$. For this set of parameters, the smallest of the inverse mean plasma gradients is $L = \langle|\nabla n_e/n_e|\rangle^{-1} = 0.35\,\mathrm{m}$, which results to a value $\kappa = 181.4$.

The first case amounts to NTM control in ITER, where a driven current deposition not further than 1 cm from the centre of the magnetic island is desirable [4]. Since the spatial gradients introduced by the island topology are of the same order as the ones of the standard ITER equilibrium [26], one can adopt the value of κ previously calculated. This yields $\kappa^{-1} = 0.005$, which is sufficient as a convergence rate and smaller that the minimum allowed error, and therefore asymptotic methods are applicable here with no problem. The second case concerns the effect of density fluctuations of different orders of magnitude encountered along propagation. In ITER, the spatial range of such fluctuations is expected to vary within $[1, 20]$ cm [28]. With a calculation like above, one finds the range of values of κ in the vicinity of the fluctuation to be $[5.6, 99.2]$. It is clear that, in this problem, asymptotic methods are quasivalid in the sense described above.

In connection to what has been presented so far, a discussion should be made on the weakly-inhomogeneous plasma description adopted by asymptotic methods. In applications, the response to EC waves is described within the infinite and homogeneous plasma theory [3, 6]. The weak variation for high-frequency waves allows to use that formula for the linear plasma tensor as a function of the spatial profiles, i.e., a transition from $\tilde{\varepsilon}(\bar{r}, B_0, n_e, T_e)$ to $\tilde{\varepsilon}[B_0(\bar{r}), n_e(\bar{r}), T_e(\bar{r})]$. This description remains valid as long as $\langle f_0^{-1}|\nabla f_0|\rangle \ll 1$, which allows for the spatial derivatives of f in (16) to be ignored. If one puts Maxwell's distribution as f_0, the result $\langle f_0^{-1}|\nabla f_0|\rangle = \langle n_e^{-1}|\nabla n_e|\rangle$ appears. Hence, the criterion for f_0 is similar to the short-wavelength limit, and so it could break down in the presence of steep plasma gradients or intrinsic flux surface geometry. In such problems, there may be further effects due to the plasma inhomogeneity and boundedness, the neglect of which may not be possible to justify. In order to remain within the plasma medium description, a novel theory for the dielectric tensor is then required which will include the terms involving ∇f in (16) (an implementation in this direction has been presented in [29]).

4. APPLICABILITY OF THE COLD PLASMA DESCRIPTION AT HIGH TEMPERATURES

Advanced asymptotic codes describe the propagation of high-frequency waves in the tokamak under different approximations for the plasma dielectric response [21–23]. Even though the plasma description plays a major role in the treatment, frequently it is very simplified. The primary simplification is the adoption of a linear plasma response. In general, this is a reasonable approximation since the waves used in

fusion applications have amplitudes much smaller than the limit for the appearance of nonlinear effects [1, 2]. However, this could break down in some cases of high-power ECRH (e.g., 20 MW in ITER) or in diagnostics utilizing narrow focused beams, due to the fact that the beam energy density may become very high [18]. There, the plasma response may be computed with models based on nonlinear kinetics, like particle tracing [8] or distribution function mapping [18, 30]. In this paper, we focus on the limitations of the models within the linear tensor description and do not refer to those cases extensively.

In almost all the asymptotic codes available for EC waves, the cold plasma dispersion function is utilized as the Hamiltonian for computing the propagation, and the cyclotron damping is calculated from the imaginary solution of the hot plasma dispersion relation, which defines the wave absorption coefficient. Hot plasma effects on the propagation due to the thermal particle motions, in most cases, are not considered. This is the essence of the weak absorption limit mentioned above, below which the imaginary wavenumber is much smaller than the refraction index, even within the resonance region, an ordering that allows the decoupling of the dispersion and absorption processes. Furthermore, the plasma is much often considered weakly-relativistic (e.g., in ITER the average temperature will be around 10 keV, equivalent to $\gamma=1.01$ or $\langle \mathrm{v} \rangle = 0.1c$), and the absorption coefficient is calculated much easier from the weakly-relativistic version of (17).

However, in many circumstances it is possible that the computed ray/beam propagation differs significantly if hot plasma effects are taken into account in the dispersion over all the plasma region. These cases are beyond the weak absorption limit, in the sense that the real and imaginary part of the wavenumber become comparable. We should note here that this does not occur due to any breakdown of the weak-inhomogeneity limit, but because the values of the plasma temperature yield a much larger anti-Hermitian part of the dielectric tensor. There are relevant results in the literature [31], and the importance of such effects in modern reactors like ITER and DEMO still has to be determined. For this task, an asymptotic code should be developed/upgraded following the path set by [10] for the derivation of the hot-plasma Hamiltonian (this is under current development).

Apart from the aforementioned, there may be further effects due to the underestimation of the importance of the relativistic factor. The source for such discrepancy is that the classical model for cyclotron damping, or its weakly-relativistic extension, differ significantly from the relativistic one: In the nonrelativistic model, resonance occurs when one electric field component co-rotates with electrons, whereas relativistic absorption is due to the Lorentz force by the transverse

component of the wave magnetic field. In this sense, the absorption of the O-mode is a purely relativistic effect, something very important for the assessment of ITER/DEMO ECRH efficiency because the current technological limits in wave sources force the use of the mode O1. In ITER, under 10 keV core temperature, the plasma could be marginally considered as weakly-relativistic, but in DEMO studies the expected core temperature of 50–60 keV makes the relativistic absorption process a crucial issue for the accuracy of ECCD computation. This is mainly the reason why the adoption of the fully-relativistic plasma description is continuously gaining ground in wave codes [32, 33].

A last issue to mention is connected to the actual implementation of the dielectric tensor in computational practice. In (17) an infinite sum of terms, relevant to the cyclotron harmonics of all orders, is to be evaluated. The general trend when computing the response to frequencies close to the n-th harmonic is to keep only terms up to that order and ignore terms of higher order as much smaller. With respect to the plasma parameters involved, this approximation is expected to hold in smaller devices, but problems may arise in ITER and beyond. The effect of parasitic absorption from higher harmonics has been identified as a cause of reduction of the ECCD efficiency in DEMO [34]. A deeper research requires the determination of the resonance region for different harmonics using the EC resonance condition

$$\omega - k_{||}\mathrm{v}_{||} - \frac{n\omega_c}{\gamma} \approx 0 \tag{23}$$

or the calculation of the absorption coefficient as a function of the harmonics. In the first manner, the radial position of the resonance and the width of the resonance region is approximated from (23) under different assumptions for $k_{||}$, $\mathrm{v}_{||}$ and γ, and the possibility of overlapping of regions relevant to adjacent harmonics is checked for.

In this paper, the second method is followed: The radial profile of the absorption coefficient is compared for the modes O1 and O2, and the numerical results that illustrate the effect of parasitic absorption are plotted. An indicative case of perpendicular propagation is studied, where the plasma parameters are related to the current DEMO design: $r_{\mathrm{maj}} = 9.6\,\mathrm{m}$, $r_{\mathrm{min}} = 2.4\,\mathrm{m}$, $B_0(0) = 7.45\,\mathrm{T}$, $n_e(0) = 1.6 \cdot 10^{14}\,\mathrm{cm}^{-3}$, $n_e(r_{\mathrm{min}}) = 4 \cdot 10^{13}\,\mathrm{cm}^{-3}$, $T_e(0) = 52\,\mathrm{keV}$, $T_e(r_{\mathrm{min}}) = 5\,\mathrm{keV}$, and the profiles of B_0, n_e and T_e are again given by (22). In Fig. 2, we present the radial profile (a) of the absorption coefficient and (b) of the electric field amplitude, as computed from (17) and (9) respectively, for the two lowest O-mode harmonics. Evidently, the absorption coefficient for O2 attains larger values from the one for O1 all the way from the launching point to the plasma centre, which implies that the undesired damping of O2 initiates well before the prescheduled one of O1, deteriorating

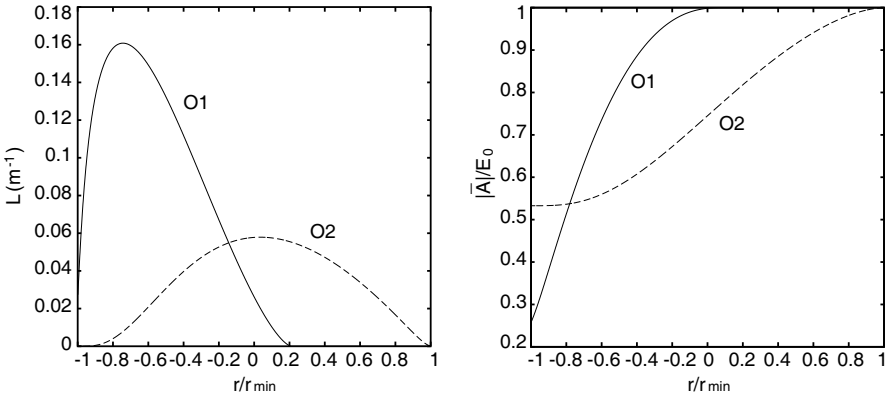

Figure 2. Visualization of the effect of parasitic absorption by higher harmonics in DEMO in terms of the radial profiles of the linear absorption coefficient and the electric field amplitude.

the goal of targeted deposition.

5. CONSISTENCY OF THE GAUSSIAN BEAM MODEL

In ECRH experiments, beams with Gaussian electric field profile are preferred because of the low Ohmic losses in the transmission line, the ease in the coupling to waveguide modes and the simplicity of modeling in theoretical studies [2]. However, beams with a non-Gaussian profile can be generated by the launching system, an undesired effect owed to a misalignment/deformation of the steering mirror due to extreme power load. Also, inside the plasma, a modification of the initial Gaussian beam shape might occur due to inhomogeneous/asymmetric absorption, caused by non-local redistribution of the wave energy by resonant particles along the magnetic field line, or to strong wave interference. In such cases, the assumption that the beam is and/or remains Gaussian may introduce an error in the description, and the modeling of the arbitrarity of the beam shape may be impositioned.

The propagation and absorption of non-Gaussian beams has been formulated in terms of the paraxial beam tracing asymptotic technique [25], as an extension to the original formulation presented in [14] for arbitrary beams that are not astigmatic. Within paraxial beam tracing, the non-Gaussian wave beam is suitably expressed as a superposition of Gaussian-Hermite modes, as given in (12). The specific sequence for the analysis is as follows: First, one assigns proper

initial conditions to all the beam-tracing variables, then solves for the reference ray, the wave-front curvature and the beam width, and finally treats the amplitude transport equation for each one of the modes. The assignment of initial conditions for the variables involved in the beam tracing equations is by no means difficult, since all these variables are calculated on the reference ray and thus are common for all the non-Gaussian modes. For the same reason, the beam tracing equations are the same for all modes. On the other hand, the amplitude transport is in general not the same for all modes, because the absorption coefficient depends on the wave-vector which is different for each mode.

The plasma volume where the power absorption takes place is partially determined by the transversal extent of the Gaussian beam. This quantity is measured by the beam width parameter, which is defined as the distance from the field maximum where a decrease of a factor of $1/e$ occurs. In the case of non-Gaussian beams, this definition may estimate wrongly the beam spot size since the field could fall below the $1/e$ limit at more than one locations along its profile. In such cases, it is necessary to generalize the width parameter already defined for the Gaussian beam, based on the moments of the amplitude distribution $|\bar{A}_0|^2(\xi_1, \xi_2)$ of the electric field in the transverse plane (ξ_1, ξ_2), defined as $\langle \xi_1^m \xi_2^n \rangle = \int_{-\infty}^{\infty} d\xi_1 d\xi_2 \xi_1^m \xi_2^n |\bar{A}_0|^2 / \int_{-\infty}^{\infty} d\xi_1 d\xi_2 |\bar{A}_0|^2$. In this frame, the generalized width is a 2-D symmetric matrix [25]

$$\tilde{W}^2 = 2 \begin{bmatrix} \langle \xi_1^2 \rangle - \langle \xi_1 \rangle^2 & \langle \xi_1 \xi_2 \rangle - \langle \xi_1 \rangle \langle \xi_2 \rangle \\ \langle \xi_1 \xi_2 \rangle - \langle \xi_1 \rangle \langle \xi_2 \rangle & \langle \xi_2^2 \rangle - \langle \xi_2 \rangle^2 \end{bmatrix} \tag{24}$$

where the subtracted terms describe any de-centering of the beam and the non-diagonal terms any coupling of the transverse directions. A special coordinate system can be found where $\tilde{W}$ becomes diagonal and its elements provide the generalized width per transverse direction.

We compute the generalized width, in comparison to the simplified $1/e$ definition, for the case of perpendicular cold-plasma propagation of a non-Gaussian EC beam in simplified ITER plasma geometry, where an analytic solution of the beam tracing equation is possible [14]. A few details on the computation are given (for a complete presentation see [25]): The plasma is confined within the region $[-r_{\min}, r_{\min}]$ along r and extends infinitely in the other two cylindrical directions z, ϕ, the magnetic field is along the z-axis and all plasma variables are functions only of r. The beam is launched from the low-field side at $r_0 = r_{\min}$ in the negative radial direction ($k_{r0} < 0, k_{z0} = k_{\phi 0} = 0$), and its electric field is the superposition of 6 Gaussian-Hermite modes, $(m, n) = (0, 0)$, $(1, 0)$, $(0, 1)$, $(1, 1)$, $(2, 0)$, $(0, 2)$, that have the same initial polarization. The mode $(0, 0)$, which describes the Gaussian part of the beam, has a circular initial profile with $1/e$-width $W_{G0} = 5$ cm and symmetric

initial focusing with curvature radius $R_{cG0} = -1.93\,\mathrm{m}$. The part of the wave power distributed over the non-Gaussian modes takes the values $e_{nG} = 0.05$ and 0.2, which correspond to a non-Gaussian content of 5% and 20% in the beam (as observed in the experiment).

In Fig. 3, the numerical results from the computation described above are visualized. In the subfigure on the left, the evolution of the $1/e$-width along propagation is plotted. The case under study corresponds to a beam injection with proper focusing such that it reaches a minimum width at a specific target point (e.g., magnetic island centre). Here the minimum width occurs near the plasma centre, which was expected according to the initial value of R_{cG}. In the subfigure on the right, the ratio of the generalized estimation for the non-Gaussian beam spot size W_{NG} over the $1/e$-width W_G is shown for the two values of e_{nG}. The difference between the two estimates appears smaller around the beam waist, probably due to the overall shrinking of the beam. A thorough scan within results from realistic cases ($e_{nG} = 0.02 - 0.25$) indicates that the ratio of the estimates varies within $[0.9, 1.6]$ overall and within $[0.9, 1.1]$ in the waist region.

The effect of the broadening of non-Gaussian beams with respect to their Gaussian approximates may play a role in the accuracy of the estimation of power damping. The power density dP/dV is inverse-proportional to the plasma volume ΔV_{abs} where the deposition occurs, which is defined as the intersection of the beam spot with the resonance region and may be approximated as a cylinder of base radius W_{NG} (see Fig. 1). Therefore, $\Delta V_{abs} \propto W_{NG}^2$ and the ratio of the different

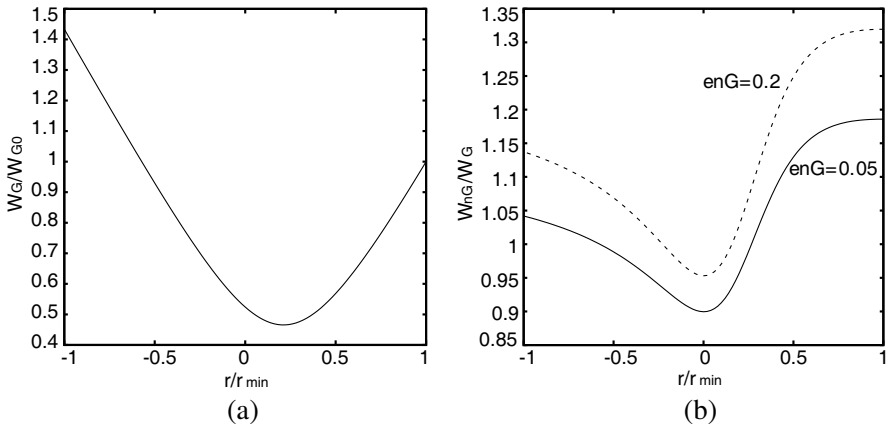

Figure 3. Non-Gaussian propagation in ITER-like geometry: Radial profile of the $1/e$-width and comparison with its generalized definition.

estimations for ΔV_{abs} is proportional to the square of W_{NG}/W_G. According to the above results, W_{NG}/W_G may vary in $[0.8, 1.2]$ at the waist region, so an estimation of ΔV_{abs} based on accepting an arbitrary beam as Gaussian may be inapproximate up to 20%, which makes possible an error in the power absorption and current drive calculation as well as to all connected estimations (e.g., NTM stabilization rate).

6. THE PROBLEM OF INACCURACY INTRODUCED BY NON-REALISTIC EQUILIBRIUM MODELS

The influence of the proper modeling of the plasma equilibrium configuration on the accuracy of ECRH/ECCD simulations should not be underestimated, since in some cases the effect of the quantities involved may be sizeable. The plasma parameters that play a role in EC wave propagation are the magnetic field (through the cyclotron frequency), the density (through the plasma frequency) and the temperature (through the thermal velocity). The reference values for these variables are normally achieved in the experiment and not subject to important changes, at least in the time-scale relevant to propagation. The stationarity of the plasma, as far as EC waves are concerned, is well-posed since the collisional and MHD phenomena evolve in a much slower time scale [5]. What is amenable to interact with the plasma dynamics, and therefore mostly approximate in wave modelling, is the radial profile and the geometry characteristics of these parameters.

The magnetic field determines the radial position of the EC resonance, and therefore geometric aspects like the Shafranov shift, elongation and triangularity should be considered when accurate prediction of the resonance zone is required. The electron density sets the wave cutoffs and causes the bending of the wave rays, whereas the temperature (together with the propagation angle) determines the width of the resonance region, so aspects like peaking or local fluctuations should be again taken into account consistently [28]. In addition, we should mention that all these parameters are present in the determination of the value of the cyclotron absorption coefficient, which is a crucial factor for the wave-plasma energy exchange. All these suggest that the capability of taking into account the actual tokamak equilibrium, in terms of a suitable method of coupling wave codes to equilibrium calculation routines, would be advantageous.

As an example, we briefly refer to the case of EC propagation in the presence of magnetic islands (one may find extensive studies on this topic in [19, 20]). The issue of relevance here is that, in most studies of ECCD-based NTM stabilization, the analysis of the propagation and deposition has been performed in terms of the unperturbed magnetic

topology, taking into account only the flux surface of interest while ignoring any effects from the islands. The basis for this assumption is that the amplitude of the magnetic perturbation is 3 orders smaller than the background field. However, the island geometry introduces differences in the plasma profiles compared to the axisymmetric case, namely a flattening of the pressure profile and a different structure of the flux surfaces, which may play a role in the wave deposition.

The EC propagation and absorption in a plasma configuration that includes magnetic islands has been computed using a ray tracing code, developed on the guidelines presented in 2, and compared to the same computation in the axisymmetric equilibrium. The non-axisymmetric magnetic configuration has been formulated by introducing a pendulum-like perturbation in the axisymmetric magnetic field, relevant to a tearing mode of order (m, n):

$$B = B_0 \left[1 + \frac{m}{n} \frac{w^2}{r_s^2} \sin\left(m\theta - n\phi\right) \right] \tag{25}$$

In the above, w is the island width, r_s the radial position of the island centre and θ, ϕ the poloidal and toroidal angle coordinates. After ray tracing, for the computation of the wave power absorption in the presence of the island, the calculation of the plasma volume between two adjacent flux surfaces is required. Following [19], the total volume V_s contained inside one flux surface is given by:

$$V_s = -\frac{1}{n} \int_0^{2\pi} \int_{\xi_1}^{\xi_2} \int_{r_1}^{r_2} \left(r_{\mathrm{maj}} + r\cos\theta\right) dr d\xi d\theta \tag{26}$$

where $\xi = m\theta - n\phi$ is the angle coordinate perpendicular to the helical line through the O-point, and r_1, r_2, ξ_1, ξ_2 are the integration limits. Based on (26) and the ray-tracing data, the absorbed power per unit volume can be evaluated as $dP/dV_s = (dP/d\tau)/(dV_s/d\tau)$.

In Fig. 4, we present results for the case of the mode $(2, 1)$ in ITER. The wave power ($P_0 = 10\,\mathrm{MW}$) is injected from the outermost flux surface with initial wavenumber calculated from the cold-plasma dispersion relation and poloidal angle such that the ray targets the O-point. The island width is $w = 20\,\mathrm{cm}$ and the toroidal angle takes the values $\phi_l = 5°$, $10.0°$, $15.0°$. On Fig. 4(a), the island topology and the ray propagation are shown. A first difference from the unperturbed case is a deviation of the ray path due to the refraction by the flattened density profile. In the part of the ray path before the O-point the deviation is in general very small, however if the launching angles are such that the ray intersection with the island is long, it might become comparable to the maximum allowed misalignment (1–2 cm). Fig. 4(b) implies that the power deposition in the presence of the island appears

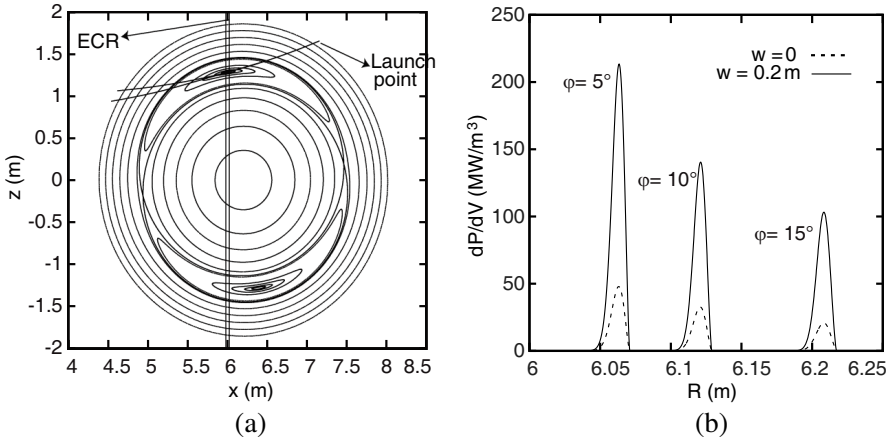

Figure 4. Illustration of the effect of magnetic island geometry on ECRH via ray tracing using a non-axisymmetric equilibrium model.

more enhanced with respect to the axisymmetric case. This is because the energy is absorbed and redistributed by the plasma particles in flux surface volumes much smaller than the ones derived when an axisymmetric topology is assumed. It is evident that, in case the effects just described are underestimated, the resulting computation provides a much different picture for the deposition, jeopardizing any effort based on this estimation.

7. CONCLUSION

High-frequency electromagnetic waves are used for plasma heating, current drive and measurements in fusion experiments. The state-of-the-art in the simulation of EC wave propagation and related effects has reached a mature state and is considered reliable for ITER modeling. There are many advanced ray-tracing codes, as well as distinguished beam-tracing codes, which describe tokamak wave propagation under different approximations for the plasma equilibrium and response. However, the inherent limitations of the asymptotic methods and the approximations in the description of the plasma, adopted by most numerical tools, limit the integrity of the simulations when more complicated effects are to be described. For such problems, more sophisticated tools should be developed in order to benchmark the validity of the simpler models, which are valuable for experiment design and control applications, and to obtain deeper physics insight.

In this work, we analyzed many of these cases where the available

modeling tools run close to or beyond the limits of their validity: (i) Plasmas appearing strong inhomogeneity in the form of localized fluctuations, steep gradients or intrinsic flux-surface geometry, for which the short-wavelength-limit is reached, (ii) high-temperature plasmas, where the cold plasma dispersion and weakly-relativistic absorption models cease to be applicable, (iii) arbitrary wave beams with sizeable non-Gaussian content, for which the consistency of the constantly-Gaussian beam assumption is lost, and (iv) special cases where a more accurate computation of the actual plasma equilibrium, or even a reconstruction from experimental data, is required.

The limitations in the currently available modeling tools, due to the adopted simplifications for the wave and plasma geometry, the plasma dynamics and the relative importance of the different processes, pose limits in the level of detail of the simulations as well as in the ability to compute more complicated effects which are expected to appear in ITER and DEMO, like, e.g., O-X-B mode conversion, nonlinear cyclotron absorption and several classes of parametric instabilities. The alternative methods to tackle such problems, which are more sophisticated, are also by far more demanding in computational resources [35]. A typical example to mention is full-wave solvers, the computational burden of which forces researchers to choose between simplifications in the geometry and/or the physics description in order to achieve realistic computer resource burden in simulations.

An additional factor that contributes to the overall uncertainty regarding the evaluation of the available models for wave propagation and plasma response dynamics is that their adequacy cannot be consistently determined, because a detailed comparison with the experiment has not been accomplished yet. In principle, this could be achieved by measuring the electron temperature response to transient ECRH power. However, there is a lack of an established method for measuring the electron temperature without introducing a major disturbance in the probed system. In exact, the ECRH power introduces a diffusive broadening of the temperature perturbations which often acts on a shorter time scale than the time resolution of the measurement. Especially if the EC power input is narrow and well localized, as, e.g., required for MHD instability suppression, the non-zero heat diffusivity makes the perturbed temperature profile broader so that it is difficult to recover the initial deposition profile.

According to the facts emerging from this work, the most prominent tool for modeling EC propagation to invest to its development should be based on extending one of the available beam tracing techniques to envisage the fully-relativistic hot plasma response

model for the computation of both the dispersion and the absorption process. At the moment, this is the most promising solution for future reactor modeling and combines simplicity, robustness and accuracy in a fairly high degree. However, an effort should be initiated for the improvement of the whole EC modeling arsenal through deeper theoretical studies and comparisons with the results of sophisticated tools, as well as of the experiment.

ACKNOWLEDGMENT

The author would like to thank Prof. K. Hizanidis, Dr. E. Poli, Dr. O. Maj, Prof. L. Vlahos, Dr. A. K. Ram and Dr. E. Westerhof for the useful discussions. This work has been sponsored by the European Fusion Programme (Association EURATOM-Hellenic Republic) and the Hellenic General Secretariat of Research and Technology. The sponsors do not bear any responsibility for the content of this work.

REFERENCES

1. Erckmann, V. and U. Gasparino, "Electron cyclotron resonance heating and current drive in toroidal fusion plasmas," *Plasma Phys. Control. Fusion*, Vol. 36, No. 12, 1869–1962, 1994.
2. Prater, R., "Heating and current drive by electron-cyclotron waves," *Phys. Plasmas*, Vol. 11, No. 5, 2349–2376, 2004.
3. Stix, T. H., *Waves in Plasmas*, Springer-Verlag, New York, 1992.
4. La Haye, R. J., "Neoclassical tearing modes and their control," *Phys. Plasmas*, Vol. 13, No. 6, Art. 055501, 2006.
5. Wesson, J., *Tokamaks*, Oxford University Press, New York, 2004.
6. Swanson, D. G., *Plasma Waves*, Taylor-Francis, New York, 2003.
7. Pinches, S. D., *The HAGIS Self-consistent Nonlinear Wave-particle Interaction Models*, UKAEA Fusion, Culham, 1998.
8. Tsironis, C. and L. Vlahos, "Effect of nonlinear wave-particle interaction on electron-cyclotron absorption," *Plasma Phys. Control. Fusion*, Vol. 48, No. 9, 1297–1310, 2006.
9. Kline, M. and I. W. Kay, *Electromagnetic Theory and Geometrical Optics*, Interscience, New York, 1965.
10. Friedland, L. and I. B. Bernstein, "General geometric optics formalism in plasmas," *IEEE Trans. Plasma Sci.*, Vol. 8, No. 2, 90–95, 1980.
11. Kravtsov, Y. I. and Y. A. Orlov, *Geometrical Optics of Inhomogeneous Media*, Springer-Verlag, Berlin, 1990.

12. Mazzucato, E., "Propagation of Gaussian beam in inhomogeneous plasma," *Phys. Fluids B*, Vol. 1, No. 9, 1855–1860, 1989.
13. Nowak, S. and A. Orefice, "Three-dimensional propagation and absorption of high frequency Gaussian beams in magnetoactive plasmas," *Phys. Plasmas*, Vol. 1, No. 5, 1242–1250, 1994.
14. Pereverzev, G. V., "Beam tracing in inhomogeneous anisotropic plasma," *Phys. Plasmas*, Vol. 5, No. 10, 3529–3541, 1998.
15. Taflove, A., *Computational Electrodynamics: The Finite-difference Tiem-domain Method*, Artech House, London, 2000.
16. Tsironis, C., T. Samaras, and L. Vlahos, "Scattered-field FDTD algorithm for hot anisotropic plasma with application to electron-cyclotron heating," *IEEE Trans. Ant. Prop.*, Vol. 56, No. 9, 2988–2994, 2008.
17. Koehn, A., A. Cappa, E. Holzhauer, F. Castejon, A. Fernandez, and U. Stroth, "Full-wave calculation of the O-X-B mode conversion of Gaussian beams in a cylindrical plasma," *Plasma Phys. Control. Fusion*, Vol. 50, No. 8, Art. 085018, 2008.
18. Kamendje, R., S. V. Kasilov, W. Kernbichler, and M. F. Heyn, "Kinetic modeling of nonlinear electron cyclotron resonance heating," *Phys. Plasmas*, Vol. 10, No. 1, 75–97, 2003.
19. Isliker, H., I. Chatziantonaki, C. Tsironis, and L. Vlahos, "Electron-cyclotron wave propagation, absorption and current drive in the presence of neoclassical tearing modes," *Plasma Phys. Control. Fusion*, Vol. 54, No. 9, Art. 095005, 2012.
20. Ayten, B. and E. Westerhof, "Consequences of plasma rotation for neoclassical tearing mode suppression by electron cyclotron current drive," *Phys. Plasmas*, Vol. 18, No. 9, Art. 092506, 2012.
21. Westerhof, E., "Implementation of TORAY at JET," Rijnhuizen Report 89-183, Eindhoven, 1989.
22. Poli, E., A. G. Peeters, and G. V. Pereverzev, "TORBEAM, a beam tracing code for electron-cyclotron waves in tokamak plasmas," *Comput. Phys. Commun.*, Vol. 136, No. 1, 90–104, 2001.
23. Farina, D., "Quasi-optical propagation of an EC Gaussian beam, absorption and current drive in tokamaks," *AIP Conf. Proc.*, Vol. 871, 77–86, 2006.
24. Lloyd, B., "Overview of ECRH experimental results," *Plasma Phys. Control. Fusion*, Vol. 40, No. 4, A119–A138, 1998.
25. Tsironis, C., E. Poli, and G. V. Pereverzev, "Beam tracing description of non-Gaussian wave beams," *Phys. Plasmas*, Vol. 13, Art. 113304, 2006.
26. Goldston, R. J. and P. H. Rutherford, *Introduction to Plasma*

Physics, IoP Publishing, Boston, 1995.

27. Maj, O., G. V. Pereverzev, and E. Poli, "Validation of the paraxial beam-tracing method in critical cases," *Phys. Plasmas*, Vol. 16, Art. 062105, 2009.
28. Tsironis, C., A. G. Peeters, H. Isliker, D. Strintzi, I. Chatziantonaki, and L. Vlahos, "EC wave scattering by edge density fluctuations in ITER," *Phys. Plasmas*, Vol. 16, Art. 112510, 2009.
29. Brunner, S. and J. Vaclavik, "Dielectric tensor operator of hot plasmas in toroidal axisymmetric systems," *Phys. Fluids B*, Vol. 5, No. 6, 1695–1705, 1992.
30. Kominis, Y., A. K. Ram, and K. Hizanidis, "Distribution functions of wave-particle interactions in plasmas," *Phys. Rev. Lett.*, Vol. 104, No. 8, 23–26, 2010.
31. Westerhof, E., "Propagation through an EC resonance layer," *Plasma Phys. Control. Fusion*, Vol. 39, No. 6, 1015–1029, 1997.
32. Ram, A. K. and J. Decker, "Relativistic effects in electron cyclotron resonance heating and current drive," *Proc. 35th EPS Conference*, Art. 1-097, 2008.
33. Farina, D., "Relativistic dispersion relation of electron cyclotron waves," *Fus. Sci. Tech.*, Vol. 53, No. 1, 130–138, 2008.
34. Poli, E., E. Fable, G. Tardini, H. Zohm, D. Farina, L. Figini, N. B. Marushchenko, and L. Porte, "Assessment of ECCD-assisted operation in DEMO," *Proc. EC-17*, Art. 01005, 2012.
35. Sirenko, K., V. Pazynin, Y. K. Sirenko, and H. Bağci, "An FFT-accelerated FDTD scheme with exact absorbing conditions for characterizing axially symmetric resonant structures," *Progress In Electromagnetics Research*, Vol. 111, 331–364, 2011.